Matrix Biology Plus 22 (2024) 100149

Contents lists available at ScienceDirect

Matrix Biology Plus

journal homepage: www.sciencedirect.com/journal/matrix-biology-plus

Binding requirements for latent transforming growth factor Beta2 activation

Nalani Sachan [a,*], Colin K.L. Phoon [b], Lei Bu [c], Lior Zilberberg [a,1], Jasimuddin Ahamed [d], Daniel B. Rifkin [a,c]

[a] Department of Cell Biology, NYU Grossman School of Medicine, New York, NY 10016, USA
[b] Department of Pediatrics, NYU Grossman School of Medicine, New York, NY 10016, USA
[c] Department of Medicine, NYU Grossman School of Medicine, New York, NY 10016, USA
[d] Cardiovascular Biology Research Program, Oklahoma Medical Research Foundation, Oklahoma City, OK 73104, USA

ARTICLE INFO

Keywords:
TGFβ2
Integrins
Latent TGFβ activation
LTBP
GARP
Heart development

ABSTRACT

Although the mechanism for activation of latent TGFβ1 and TGFβ3 is understood to involve the binding of the TGFβ propeptide (LAP) to both an integrin and an insoluble substrate, the activation of latent TGFβ2 has been unclear because the TGFβ2 LAP does not have the classical integrin binding sequence found in the other two TGFβ isoform LAPs. To assess the potential requirement for covalent linkage with a matrix or cell surface protein for the activation of latent TGFβ2, we generated mice in which the TGFβ2 Cys residue predicted to be involved in binding was mutated to Ser (*Tgfb2*^{C24S}). We reasoned that, if covalent interaction with a second molecule is required for latent TGFβ2 activation, mutant mice should display a *Tgfb2* null (*Tgfb2*$^{-/-}$)-like phenotype. *Tgfb2*^{C24S} mice closely phenocopy *Tgfb2*$^{-/-}$ mice with death in utero between E18 and P1 and with congenital heart and kidney defects similar to those described for *Tgfb2*$^{-/-}$ mice. The mutant latent TGFβ2 is secreted at levels similar to WT, yet TGFβ signaling monitored as nuclear pSmad2 is suppressed. We conclude that, like latent TGFβ1, latent TGFβ2 activation requires binding to an immobilized matrix or plasma membrane molecule.

Introduction

The multifunctional cytokine transforming growth factor beta (TGFβ) includes three mammalian isoforms: TGFβ1, -β2, and -β3 [1,2]. These isoforms are synthesized as dimers and are cleaved by furin. They are secreted as part of inactive latent complexes consisting of the 25-kDa disulfide-bonded mature TGFβ homodimer and the cleaved N-terminal TGFβ propeptide dimer, called latency-associated peptide (LAP), which together form the small latent complex (SLC) [3,4]. Within the SLC, LAP envelops the mature TGFβ preventing binding with its receptor, thereby conferring latency. Most SLC is secreted in a form in which the LAP is disulfide bonded to either a latent TGFβ binding protein (LTBP) or transmembrane glycoprotein-A repetitions predominant (GARP) molecule [3,5–8]. This tripartite complex is called the large latent complex (LLC). To bind to its receptor, the mature cytokine must be released or uncovered from the complex by a process called activation. Several conditions or molecules, including proteases, thrombospondin-1, reactive oxygen species, integrins, or shear force, facilitate latent TGFβ activation in vitro [3,9,10]. Among these processes, activation by integrins has been characterized most extensively [3,11,12]. Both TGFβ1 and TGFβ3 LAP contain the integrin binding sequence Arg–Gly–Asp (RGD), allowing the integrins of the α_V class including $\alpha_V\beta_1$, $\alpha_V\beta_3$, $\alpha_V\beta_5$, $\alpha_V\beta_6$, and $\alpha_V\beta_8$ to activate by a proposed traction mechanism that distorts the latent complex permitting ligand binding to its receptor [11–16]. This mechanism presumes that the SLC is tethered to either an LTBP molecule crosslinked to the matrix or to a transmembrane GARP molecule. The integrin $\alpha_V\beta_8$ is unique among the integrin activators as it can bind soluble SLC, which has no LTBP, and activate the latent TGFβ [17,18].

Mice expressing TGFβ1 LAP with a mutation of Arg–Gly–Asp to Arg-Gly-Glu have a phenotype congruent with TGFβ1 knockout mice, indicating that integrin-mediated activation is crucial for latent TGFβ1 activation in vivo [19]. Likewise, mice with a Cys to Ser mutation in the TGFβ1 LAP residues that bind to LTBP or GARP display a *Tgfb1* null-like phenotype, implying that LLC formation is also essential for latent TGFβ1 activation [20]. These results are consistent with a model in

* Corresponding author.
E-mail address: Nalani.Sachan@NYUMC.org (N. Sachan).
[1] Current address: Smidt Heart Institute, Cedars-Sinai Medical Center, Los Angeles, CA, 90048, USA.

https://doi.org/10.1016/j.mbplus.2024.100149
Received 23 January 2024; Received in revised form 15 April 2024; Accepted 11 May 2024
Available online 14 May 2024

which the LLC bound to the extracellular matrix or GARP allows the integrin to exert force on the immobilized LLC, thereby distorting the complex and thus permitting the mature cytokine to bind to its receptor [15,16,21].

TGFβ2 LAP does not contain an Arg–Gly–Asp sequence and thus the mechanism of latent TGFβ2 activation has been unclear [12,13]. Recently, Le et al. reported that the integrin $\alpha_V\beta_6$ can activate latent TGFβ2 produced by cells grown in culture if the cells also expressed GARP [22]. However, it was not clear if this mechanism is used in vivo. We reasoned that if a force-dependent reaction was required for the activation for latent TGFβ2, similar to that described for latent TGFβ1, a Cys to Ser mutation of the TGFβ2 LAP Cys residues analogous to those in TGFβ1 LAP that bind to LTBP should yield mice with a *Tgfb2* null phenotype. Here we show that *Tgfb2*^{C24S} mice have a phenotype similar to that of *Tgfb2*$^{-/-}$ animals with impaired kidney and heart development, as well as neonatal lethality. Cells from the mutant animals secrete TGFβ2 SLC at levels comparable to that of WT cells, but TGFβ signaling is reduced. These results imply that activation of latent TGFβ2 requires the formation of an LLC and probably the application of force similar to that required for activation of TGFβ1 and TGFβ3 LLCs.

Results

Secretion of TGFβ2^{C24S}

To demonstrate that the Cys residue at position 24 in the TGFβ2 LAP was required for disulfide bonding to LTBP, we mutated the *Tgfb2* cDNA Cys codon at residue 24 to Ser and expressed the pEF6 constructs in HEK cells and analyzed the secreted TGFβ2. Immunoblotting of proteins in the serum free-conditioned medium (SF-CM) from cells transfected with either WT *Tgfb2* or *Tgfb2*^{C24S} expression constructs and probed using an antibody against TGFβ2 LAP indicated that both WT and mutant proteins were secreted (Sup. Fig. 1). The two bands at 100 and 75 kDa represent the unprocessed TGFβ2-LAP precursor and the TGFβ2 LAP dimer, respectively. Coexpression of LTBP3 plus a WT TGFβ2 construct resulted in the formation of a high molecular weight band of approximately 250 kDa. This is presumably TGFβ2 in a covalent complex with LTBP3. This band was not observed in the SF-CM from cells co transfected with LTBP3 and *Tgfb2*^{C24S} constructs indicating that the Cys residue at position 24 is the amino acid in the TGFβ2 LAP that binds to LTBP3.

We also tested the potential signaling activity of the secreted mutant TGFβ2 by heating SF-CM from HEK cells that were stably transfected with either WT *Tgfb2* or *Tgfb2*^{C24S} expression constructs plus an *Ltbp3* expression construct, and measuring the cytokine activity with a cell-based assay. The results of the assay indicate that transfected cells expressing either WT *Tgfb2* or *Tgfb2*^{C24S} secrete TGFβ in similar amounts (Fig. 1). The signaling activity of the heated SF-CM was blocked by the addition of a TGFβ2 neutralizing antibody or the pan neutralizing antibody 1D11 indicating that TGFβ2 was present. A TGFβ1 neutralizing antibody had almost no effect on the activity indicating that most of the measured activity in the media was TGFβ2. The combination of anti-TGFβ1 and anti-TGFβ2 antibodies also resulted in an almost total inhibition of the signal showing that the majority of the activity was TGFβ2 with some TGFβ1. The residual activity after treatment of SF-CM with both TGFβ1 plus TGFβ2 neutralizing antibodies might be TGFβ3. However, this was not tested directly as the remaining activity was quite small indicating that any existent TGFβ3 activity was minor. The TGFβ1 antibody did not block the activity of recombinant (Rcb) TGFβ2 and the TGFβ2 antibody neutralized Rcb TGFβ2. These results indicate that the mutant TGFβ2 SLC is secreted, can be activated, and the active TGFβ2 can signal in a bioassay.

Preparation of Tgfb2^{C24S} *mice*

We utilized the CRISPR-Cas9 strategy described in Methods to introduce a mutation changing Cys 24 to Ser in the endogenous *Tgfb2* (NM_009367) gene. Founder mice were identified as described in Methods. Two offspring lines containing the mutation were chosen for further study. The DNA sequence of the nucleotides surrounding the putative change revealed the expected mutated sequence (Sup. Fig. 2). In addition to finding no mutations within the TGFβ2 LAP binding region, the phenotypes of the two founder lines remained constant over more than five years indicating that a second mutation on a chromosome other than that containing the TGFβ2 gene was unlikely, as such a mutation would have segregated out over time due to chromosomal exchange during breeding.

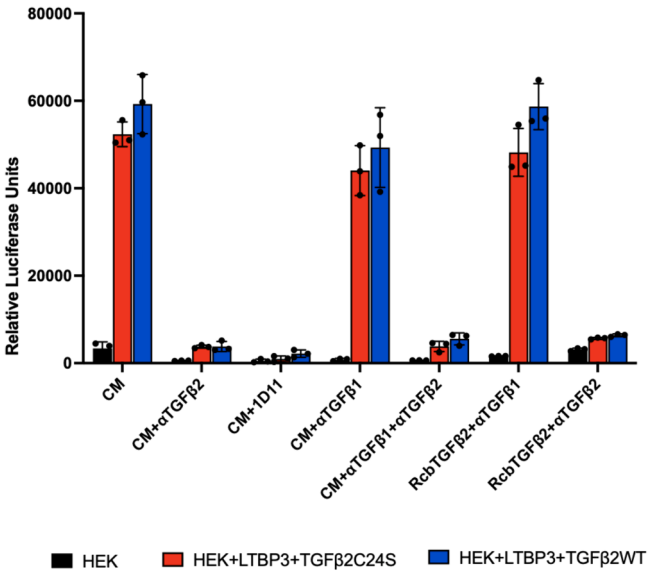

Fig. 1. TGFβ isoforms produced by HEK cells transfected with WT *Tgfb* and *Tgfb2*$^{C24S/C24S}$ expression vectors. SF-CM from either WT HEK cells or cells expressing *Tgfb2*$^{C24S/C24S}$ or *Tgfb2*$^{Wt/Wt}$ plus *Ltbp3* were heated to activate latent TGFβ and treated with a pan TGFβ neutralizing antibody (1D11), a TGF2 specific neutralizing anti body, or recombinant TGFβ1 or 2 plus antibodies as indicated in the figure. The medium was subsequently assayed for TGFβ activity. The results indicate that essentially all of the activity was TGFβ2 (n = 3 biological replicates and n = 2 technical replicates).

An analysis of the genotypes of pups from intercrosses of *Tgfb2*$^{WT/C24S}$ mice indicated that no homozygous mutant mice survived to P15 (Table 1). Analysis of two litters immediately after birth revealed two dead *Tgfb2*$^{C24S/C24S}$ pups but no surviving *Tgfb2*$^{C24S/C24S}$ mice. Analysis of embryos from timed pregnant dams revealed that by E18.5 most of the *Tgfb2*$^{C24S/C24S}$ embryos had died (Table 1), but at E14.5 the distribution of genotypes was in the expected Mendelian ratio of 1:2:1 (Table 1). Interestingly, when *Tgfb2*$^{-/-}$ mice were examined, there were no live births and by E18.5, only four of seventy-one embryos were alive. The number of live embryos at E14.5 was not determined.

Tissue analysis of Tgfb2^{C24S} *mice*

Congenital Heart Defects – *Tgfb2*$^{-/-}$ mice have multiple abnormalities in heart development including ventricular and atrial septal defects (VSD and ASD), double-outlet right ventricle, double-inlet left

Table 1
Genotypes of *Tgfb2*$^{WT/C24S}$ Intercrosses.

Age	Genotype		
	Wild Type	***Tgfb2*$^{+/C24S}$**	***Tgfb2*$^{C24S/C24S}$**
P15	157/460 (34.1 %)	303/460 (65.9 %)	0/460 (0 %)
E18.5	13/32 (40.6.%)	18/32 (56.3 %)	1/32 (3.1 %)
E14.5	30/112 (26.7 %)	52/112 (46.4 %)	30/112 (26.7 %)

ventricle, and truncus arteriosus [23]. When we compared 5 μm H&E-stained transverse sections of E14.5 wt, *Tgfb2*$^{C24S/C24S}$ and *Tgfb2*$^{-/-}$ embryo hearts, we observed a number of abnormalities common to both *Tgfb2*$^{C24S/C24S}$ and *Tgfb2*$^{-/-}$ null embryos. VSDs were frequent (23/23 embryos) in both *Tgfb2*$^{C24S/C24S}$ and *Tgfb2*$^{-/-}$ embryos (Fig. 2A). In addition, examination of the ventricular walls revealed that mutant embryos of both genotypes exhibited both a thinner compact myocardium and more disorganized and reduced trabecular myocardial layer compared to WT (Fig. 2B). *Tgfb2*$^{C24S/C24S}$ embryos also had frequent ASDs (5/6 embryos) by E14.5 (Fig. 3). We observed additional congenital heart defects in *Tgfb2*$^{C24S/C24S}$ embryos including truncus arteriosus (1/12 embryos) and double-outlet right (6/23 embryos) or double-inlet left (7/23 embryos) ventricles, but these two abnormalities were not as frequent as VSD and ASD.

Kidney – At E14.5 in H&E stained sections (3 μm), we detected an enlarged renal pelvis in E14.5 *Tgfb2*$^{C24S/C24S}$ embryos compared to WT embryos (Fig. 4). An enlarged renal pelvis defect was reported at E18.5 *Tgfb2*$^{-/-}$ embryos [24]. We did not observe this in our *Tgfb2*$^{-/-}$ embryos at E14.5, but the defect was evident by E16.5 (Fig. 4). The numbers of animals with enlarged renal pelvis were 0/8 for WT mice at E14.5, 8/10 for *Tgfb2*$^{C24S/C24S}$ mice at E14.5, 0/7 for *Tgfb2*$^{-/-}$ mice at E14.5, and 4/7 for *Tgfb2*$^{-/-}$ mice at E16.5.

The more severe phenotype of *Tgfb2*$^{C24S/C24S}$ compared to *Tgfb2*$^{-/-}$embryos may be a reflection of differences in the backgrounds of mice used in our studies as well as the animals used in the original studies with *Tgfb2*$^{-/-}$ mice [25].

Secretion of TGFβ2^{C24S}

The similarities of *Tgfb2*$^{-/-}$ and *Tgfb2*$^{C24S/C24S}$ embryo phenotypes could represent an impairment of TGFβ2^{C24S} secretion that would mimic the *Tgfb2*$^{-/-}$ phenotype. Although the experimental results illustrated in Fig. 1 and Sup. Fig. 1 indicate that TGFβ2^{C24S} was secreted efficiently by HEK cells, we wished to establish if this was also true for cultured *Tgfb2*$^{C24S/C24S}$ mouse embryonic fibroblasts (MEF). Immunoblotting analysis of TGFβ2 secreted by WT and *Tgfb2*$^{C24S/C24S}$ MEFs indicated that similar amounts of both mature ligands, as measured by the corresponding LAP, were secreted from both cell types (Fig. 5A and B). However, there was little reactivity at the position of the LLC in the SF-CM from the mutant cells. The small amount of staining might represent LLC from the serum used in the MEF cultures. When the bands from the gel in Fig. 5A were scanned, the only bands that showed a statistical difference between WT and mutant were the bands representing the LLC, as would be expected from the nature of the mutation (Sup. Fig. 3). To establish that the secreted latent TGFβ2^{C24S} could signal if activated, we measured total TGFβ activity of heat-treated samples of SF-CM in the presence and absence of an antibody that neutralizes all isoforms of TGFβ as well as an antibody specific for TGFβ2 (Fig. 5C). WT and mutant samples had similar total TGFβ activities (Fig. 5C). The values registered after incubation with either a pan neutralizing antibody (1D11) or an anti TGFβ2 specific antibody showed similar levels of suppressed TGFβ activity in the SF-CM of WT compared to mutant samples. The residual activity in the conditioned medium after incubation with the anti-TGFβ2 specific antibody probably represents TGFβ1 or 3. This was not investigated. Therefore, both WT and *Tgfb2*$^{C24S/C24S}$ cultured MEF secreted approximately equivalent amounts of TGFβ2.

Although the results from the experiments in the preceding section indicated that the Cys to Ser mutation had no effect on TGFβ2 secretion by MEFs, we also examined TGFβ2^{C24S} secretion in vivo using immunohistochemistry. We probed formalin fixed non-permeabilized tissue sections from E16.5 kidneys for extracellular TGFβ2 LAP using a TGFβ2 LAP-specific antibody. The results indicate significant amounts of extracellular immuno-reactive material in the sections from both WT and *Tgfb2*$^{C24S/C24S}$ embryos but no staining in sections from *Tgfb2*$^{-/-}$ kidneys (Fig. 6). This result implies that the *Tgfb2*$^{C24S/C24S}$ phenotypes are not the result of insufficient secretion of the mutant cytokine. Taken together, the comparable levels of TGFβ2 secreted from HEK cells (Fig. 1) and MEFs (Fig. 5B), as well as the IHC data indicate that secretion of the mutant TGFβ2 is normal and insufficient secretion cannot explain the *Tgfb2*$^{C24S/C24S}$ phenotypes.

TGFβ signaling in Tgfb2$^{C24S/C24S}$ *mice*

The phenotypes of *Tgfb2*$^{C24S/C24S}$ mice imply defective TGFβ2 signaling, since there appeared to be no significant deficit in TGFβ2 secretion. To support this contention, we examined embryonic kidney sections from WT, *Tgfb2*$^{C24S/C24S}$ and *Tgfb2*$^{-/-}$ embryos for impaired TGFβ signaling by staining for the surrogate TGFβ signaling marker pSmad2. The results indicate significantly reduced levels of pSmad2 in *Tgfb2*$^{C24S/C24S}$ and *Tgfb2*$^{-/-}$ samples compared to the WT (Fig. 7). To quantify the results from Fig. 7, we scanned the samples and determined the amount of nuclear pSmad2 (Sup. Fig. 4). This result is consistent

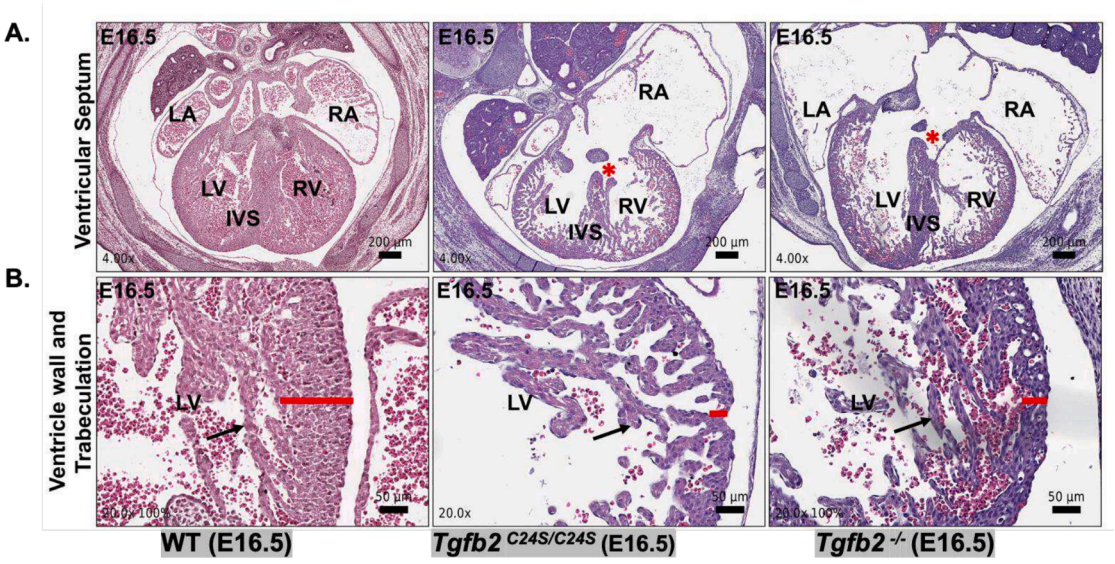

Fig. 2. H&E stained E16.5 mouse embryonic heart cross-sections of WT, *Tgfb2*$^{C24S/C24S}$, and *Tgfb2*$^{-/-}$ embryos. (A) *Tgfb2*$^{C24S/C24S}$ and *Tgfb2*$^{-/-}$ hearts with ventricular septal defects (VSD; *). (B) Thinner ventricular walls (-); disorganized and reduced trabeculation () in *Tgfb2*$^{C24S/C24S}$ and *Tgfb2*$^{-/-}$ embryos compared to WT. LA, left atrium; RA; right atrium; LV, left ventricle; RV, right ventricle; IVS, inter ventricular septum.

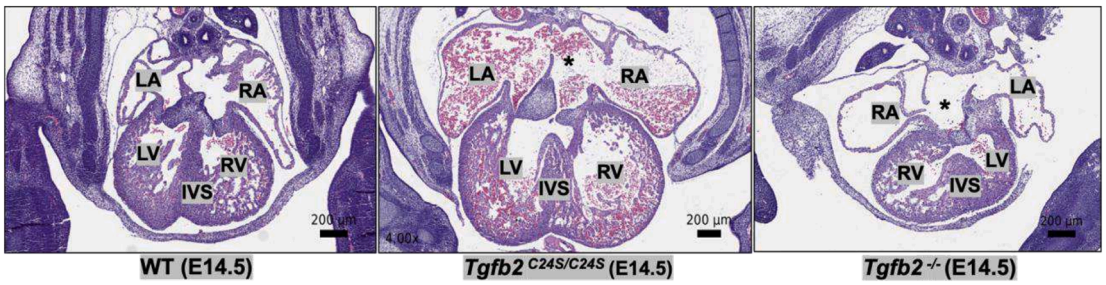

Fig. 3. H&E stained E14.5 mouse heart cross-sections from WT, *Tgfb2*$^{C24S/C24S}$ and *Tgfb2*$^{-/-}$ embryos. *Tgfb2*$^{C24S/C24S}$ and *Tgfb2*$^{-/-}$ embryos have atrial septal defects as indicated by the *. LA, left atrium; RA; right atrium; LV, left ventricle; RV, right ventricle; IVS, interventricular septum; (*) atrial septal defect.

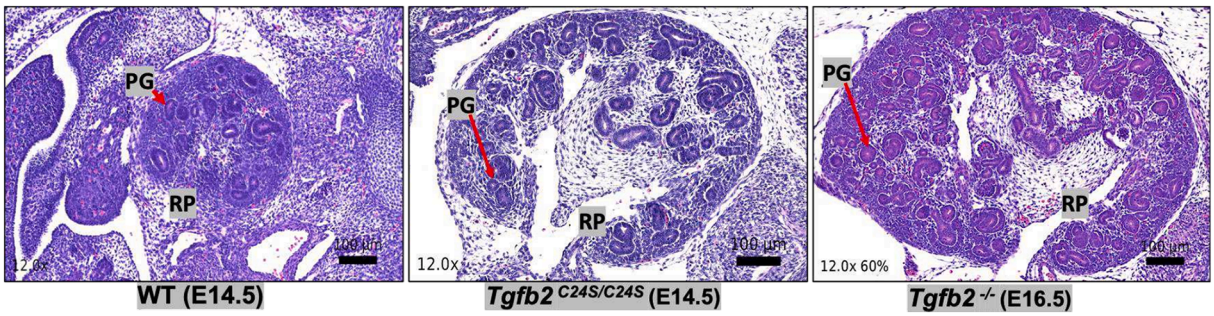

Fig. 4. H&E-stained mouse embryonic kidney cross-sections of WT (E14.5), *Tgfb2*$^{C24S/C24S}$ (E14.5), and *Tgfb2*$^{-/-}$ (E16.5) embryos. *Tgfb2*$^{C24S/C24S}$ and *Tgfb2*$^{-/-}$ embryos have enlarged renal pelvis. PG: primitive glomeruli; RP: renal pelvis.

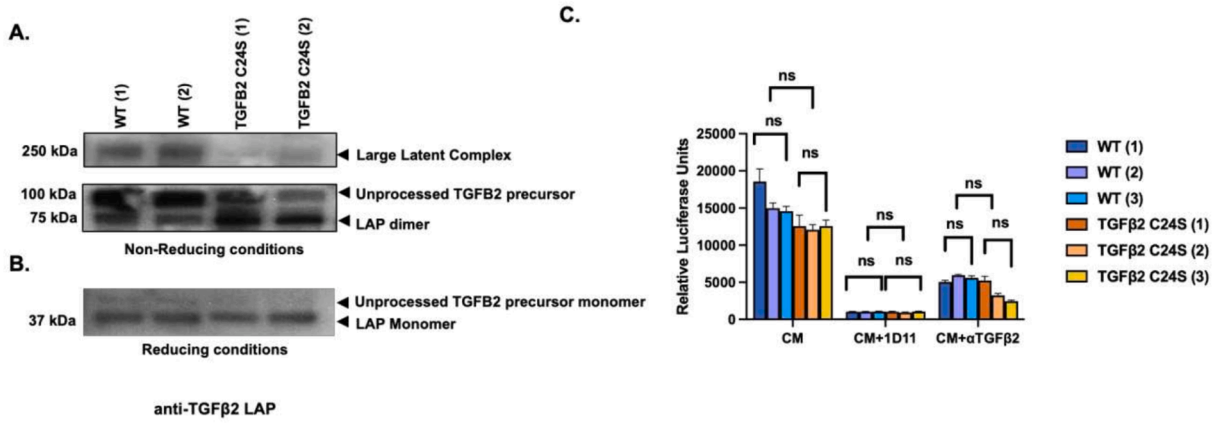

Fig. 5. Immunoblotting and activity of secreted latent TGFβ2 complexes from WT and *Tgfb2*$^{C24S/C24S}$ E14.5 MEF SF-CM. A. Immunoblotting under non-reducing conditions, B. Immunoblotting under reducing conditions. C. Measurement of TGFβ activity in WT and TGFβ2 MEF SF-CM. Total TGFβ activity was measured in SF-CM that was heated and incubated with an antibody (1D11) that neutralizes all TGFβ isoforms or with an antibody that neutralizes only TGFβ2, and assayed (n = 3 biological replicates and n = 3 technical replicates). Results are represented as RLU.

with a deficit in latent TGFβ2 activation in the mutant mice as there is a minimal amount of signaling even though the results from Fig. 6 indicate that significant amounts of the growth factor are secreted.

Discussion

The goal of these experiments was to discern if the mechanism for effective latent TGFβ2 activation required covalent bonding to an anchoring molecule via a Cys residue in the TGFβ2 LAP. Latent TGFβ1 and TGFβ3 are thought to be activated primarily via a force dependent mechanism in which an integrin binds to an RGD sequence in LAP and exerts force thereby distorting the complex, which is tethered to the matrix or cell membrane [26]. This change in conformation of the complex permits the mature TGFβ to bind to its receptor. However, the TGFβ2 LAP does not have the canonical Arg–Gly–Asp sequence recognized by integrins known to activate latent TGFβ1 and TGFβ3 [3,11,12]. This failure to activate latent TGFβ2 with various integrins in vitro has raised the question of whether latent TGFβ2 utilizes an activation process different from that of latent TGFβ1 and TGFβ3. Earlier experiments with TGFβ1 indicated that formation of an LLC was crucial for conversion of latent to active TGFβ1, as mutation of the TGFβ LAP Cys residue that binds to an LTBP or a GARP yielded animals that phenocopy *Tgfb1*$^{-/-}$ mice [10,19,20,27]. Here we show that mice with a Cys to Ser mutation at residue 24 in TGFβ2 LAP present with a phenotype that closely resembles that of *Tgfb2*$^{-/-}$ mice with early lethality, as well as kidney and heart developmental defects. The mutant protein is secreted from cells in vitro and in vivo, but there is little to no TGFβ signaling, as monitored by kidney pSMAD2 levels. These data indicate that latent

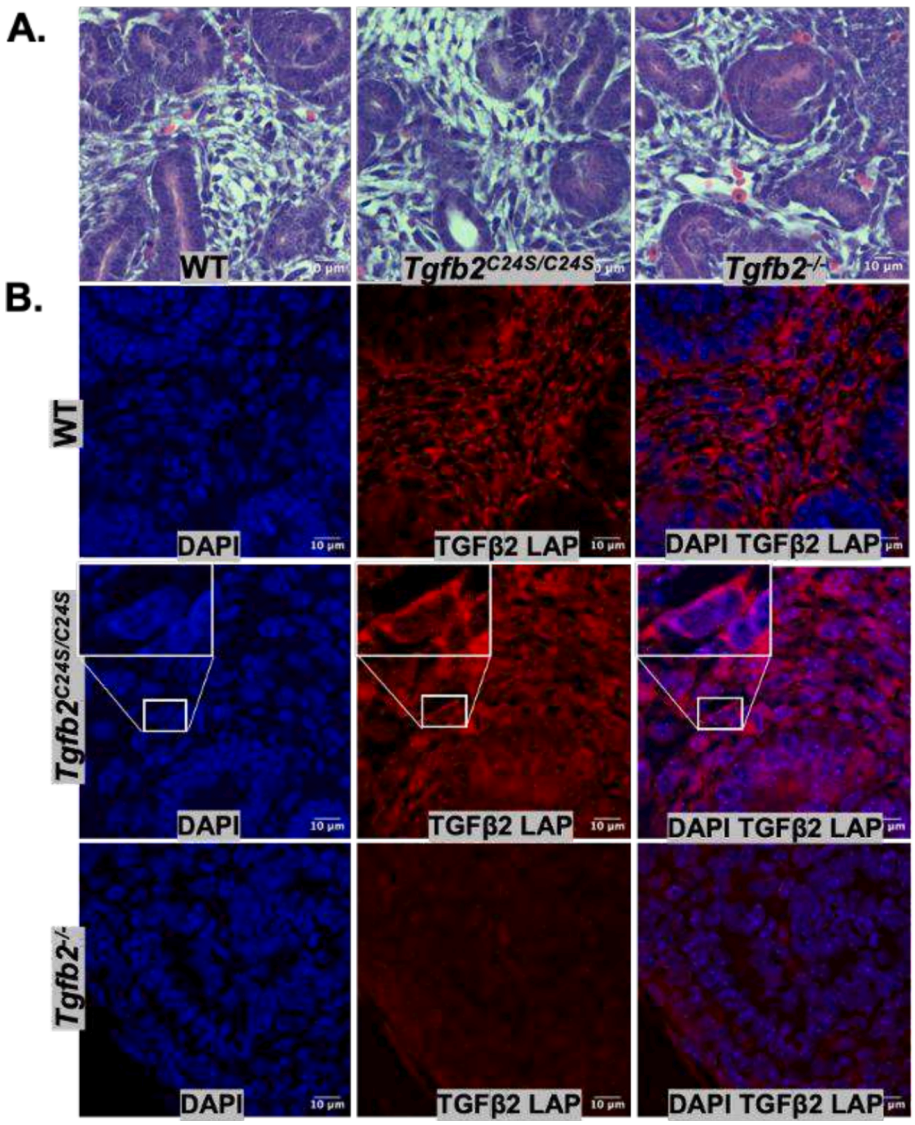

Fig. 6. TGFβ2 LAP secretion in E16.5 mouse embryonic kidney cross-sections. (**A**) H&E-stained cross-sections of WT, *Tgfb2*$^{C24S/C24S}$ and *Tgfb2*$^{-/-}$ kidneys. (**B**) Immunofluorescence of TGFβ2 LAP in WT, *Tgfb2*$^{C24S/C24S}$ and *Tgfb2*$^{-/-}$ kidneys. Fluorescence from TGFβ2 LAP is located around DAPI positive cells in the WT and *Tgfb2*$^{C24S/C24S}$ samples but is absent from the *Tgfb2*$^{-/-}$ samples. Inset indicates higher (3×) magnification of the indicated regions.

TGFβ2 activation is similar to that of latent TGFβ1 and requires the formation of an LLC for efficient activation.

We are confident that the phenotypes we observed are the result of the Cys to Ser mutation for several reasons. First, DNA sequencing of the region indicated that the proper mutation was present. Second, it is unlikely that a mutation at another site impeded TGFβ2 secretion or activation because the mice have retained the phenotype for over 5 years. Secondary mutations on another chromosome or even reasonably close to the targeted site would have been lost by chromosome segregation or crossing over if this were the case. Third, latent TGFβ2 is secreted by cells at normal levels indicating the phenotype is not the result of an impairment in protein secretion. Fourth, the secreted mutant latent TGFβ2 can be activated by heating, binds to its receptor, and signals. Therefore, there appears to be no effect of the mutation on the mature cytokine. However, the unambiguous demonstration of the lack of a secondary mutation causing an effect would require solving the three-dimensional structure of the mutant protein and additional information on the activation mechanism.

Although the *Tgfb2*$^{C24S/C24S}$ mice resemble *Tgfb2*$^{-/-}$ mice, they are not identical. This probably reflects the fact that different mouse strains were used; we used C57Bl6J mice, whereas the *Tgfb2*$^{-/-}$ mice were on a 129/Sv x Black Swiss background maintained by brother/sister mating. In the original publication characterizing *Tgfb2*$^{-/-}$ mice, the animals were in a 129/Sv/Black Swiss F1 background [25]. *Tgfb2*$^{-/-}$ mice on the 129/Sv/Black Swiss F1 background survived to birth, whereas *Tgfb2*$^{-/-}$ mice as we maintained them did not survive to birth. Indeed, *Tgfb1*$^{-/-}$ animals on a pure C57Bl6J background are known to have a stronger penetrance of the phonotypes than outbred animals [25].

Our data are consistent with an activation mechanism for latent TGFβ2 similar to that of TGFβ1 and TGFβ3 involving the binding of LAP to a matrix or cell membrane component and distortion of the latent complex by the application of force via integrin binding to a site on LAP. The effect of the force is dependent upon the attachment of the LLC either to the extracellular matrix or to a transmembrane protein (GARP). In this model, failure of the SLC to be anchored would prevent the transmission of force within the latent complex resulting in a lack of active TGFβ generation. At the present time we have no way of distinguishing if an LTBP or GARP is involved in latent TGFβ2 activation in the tissues we examined. We also only tested the binding of the TGFβ2 SLC to LTBP3 and did not measure binding to LTBP1 or LTBP4. LTBP4 was reported to bind only TGFβ1 [12]. However, published biochemical evidence is consistent with LTBP1 and 3 binding to the TGFβ2 SLC in an identical manner [12].

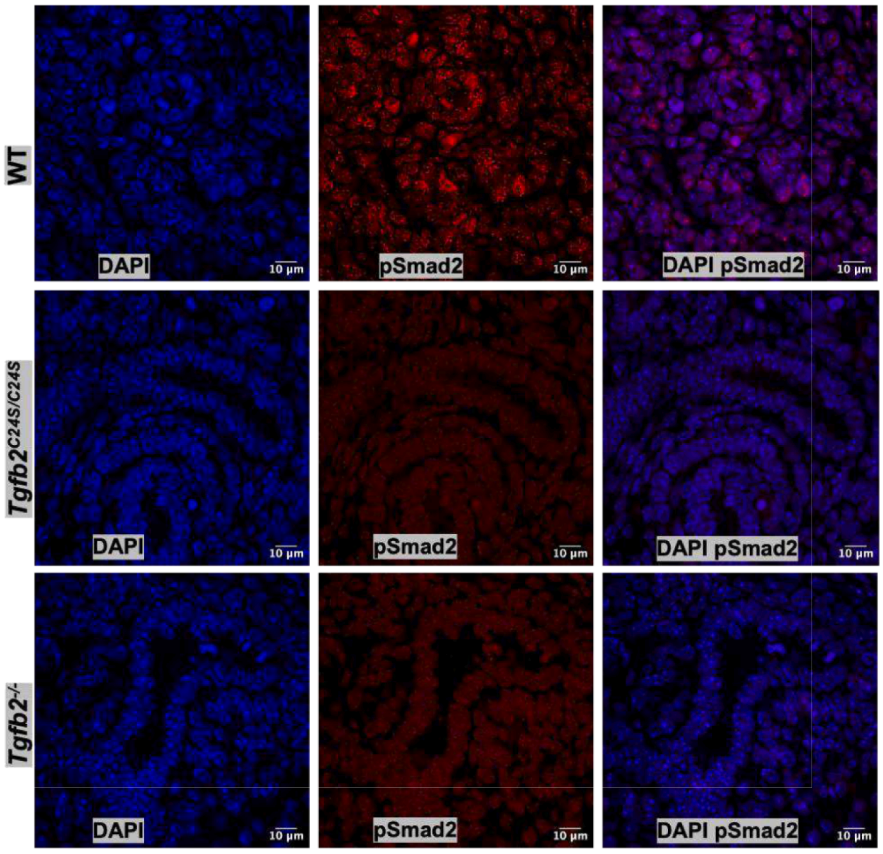

Fig. 7. Psmad2 immunofluorescence in wt,*Tgfb2*$^{C24S/C24S}$, and *Tgfb2*$^{-/-}$ E16.5 mouse embryonic kidney cross-sections. pSmad2 reactivity is present in the WT sample, but is absent in both mutant samples, indicating a lack of TGFβ signaling.

It is interesting to note that the amount of bound extracellular LAP is roughly equivelent in WT and mutant kidney tissue even though the mutant SLC has no LTBP, which is thought to bind to the matrix (Fig. 6). We do not know the reason for this, but the binding properties of LAP or SLC to matrix proteins have not been studied.

Earlier failures to observe latent TGFβ2 activation by integrins may have reflected the absence or insufficient levels of LAP binding anchors, as $\alpha_v\beta_6$ was recently reported to support the activation of latent TGFβ2 when co expressed with GARP or LTBP [22]. Our results are consistent with this integrin-based mechanism for latent TGFβ2 activation by demonstrating a requirement for tethering of LAP. TGFβ2 LAP does have Ile-Asp-Gly sequence in a position similar to that of the Arg-Glu-Asp in TGFβ1 and TGFβ3 LAPs and this sequence is recognized by the integrin $\alpha_9\beta_1$ [28]. However, $\alpha_9\beta_1$ deficient mice do not recapitulate the phenotype of TGFβ2 null mice nor did we find that $\alpha_9\beta_1$ was capable of activating latent TGFβ2 in vitro [29,30]. However, our experiments were not performed with co-expression of a LAP anchoring protein. It would be interesting to test if enhanced availability of GARP or LTBP promoted latent TGFβ2 activation by $\alpha_9\beta_1$.

It is known that the integrin $\alpha_V\beta_8$ can activate TGFβ1 SLC [17]. Therefore, we were concerned that activation of the SLC of the mutant TGFβ2 by $\alpha_V\beta_8$ might compensate for the loss of the LLC. However, there was no evidence of activation of latent TGFβ2 in our experiments. In addition, $\alpha_V\beta_8$ was reported not to activate latent TGFβ2 in vitro [22].

Although we believe that the activation mechanism perturbed in *Tgfb2*$^{C24S/C24S}$ mice is one involving force, we cannot rule out that a normally utilized proteolytic activation process is not blocked by the amino acid change introduced in the TGFβ2 LAP by the substitution of Ser for Cys. Nor can we be certain that different activation mechanisms are not employed at different stages of development or growth. We also cannot rigorously rule out an effect on pro TGFβ processing in tissues. However, at this time there are no data suggesting either different in vivo and in vitro processing or secretion properties regarding mutant vs. WT TGFβ1 or 2 when binding to an LTBP is prevented. Resolution of these points awaits the availability of additional information regarding activation as well as mice with conditional TGFβ2 mutations.

The fact that an effective in vitro system for latent TGFβ2 activation has not been described has severely impeded progress in understanding the control of TGFβ2 activity in a number of biologically important phenomena, including the development of the heart [31]. Our results support the contention that binding to an integrin or integrin-like molecule to LAP is part of the activation mechanism for latent TGFβ2 in vivo. With the availability of faster and less costly ways to make mouse germline mutations, it would be worthwhile to determine if the TGFβ2 Ile-Asp-Gly sequence is critical in vivo by making a point mutation as was done for TGFβ1 [14]. This is a long-term goal.

Methods

Mice

Tgfb2$^{C24S/+}$ mice were generated using CRISPR-Cas9 gene editing technology. CRISPR-Cas9 strategy was used to convert cysteine into serine at codon 24 of the endogenous *Tgfb2* (NM_009367) gene using C57BL/6J mice (Jax laboratory). The guide RNA (ATCCATGTCGAGGGTGCTGC) was used to target exon 1 of the *Tgfb2* gene to create double DNA strand breaks to facilitate homologous recombination using the template oligo (GCACCTTTTTGCTCCTGCATCTGGTCCCGGTGGCGCTCAGTCTGTC-TACC**TCT**AGCACCCTCGACATGGATCAGTTTATGCGCAAGAGGATCG). Guide RNAs were synthesized and purified using a MEGAshortscript™ T7

Transcription Kit (Invitrogen) and a MegaClear Kit (Ambion). Purified guide RNAs along with Cas9 mRNA (TriLink, Cat#L7206) and the C24S template oligo were injected into C57BL/6J fertilized eggs. Embryos were transferred into recipient pseudo pregnant C57BL/6J females and 35 founder pups were born. Five founders with the C24S conversion were identified via PCR and Sanger sequencing by using the following primers (forward: 5′-CTACCTGACCGCTCTGAGAAT-3′; reverse: 5′-TCCCTGGTAC TGTTGTAGATGG-3′). Founders with the correct DNA sequence were chosen for breeding and each was crossed with C57BL/6J mice. *Tgfb2*$^{+/-}$ mice were the generous gift of Dr. Thomas Doetschman (University of Arizona, Tucson, USA) [24]. When received, *Tgfb2*$^{+/-}$ mice were on a C57BlJ6 x outbred Black Swiss background. These mice were maintained by brother/sister mating. All the experiments conducted in this study were performed using a protocol approved by the Institutional Animal Care and Use Committee (IACUC) at the New York University Langone Medical Center.

Genotyping

Mouse tails (~2 mm) were lysed in 75 μl, 25 mM NaOH/0.2 mM EDTA by incubation in a thermocycler at 98 °C for 1 h, followed by reduction of the temperature to 4 °C at which time, 75 μl of 40 mM Tris HCl (pH 5.5) was added and the samples were mixed by pipetting. For genotyping of *Tgfb2*$^{+/C24S}$ mice, the WT allele was analyzed using the primers: Tgfb2-GT-Fw: CTACCTGACCGCTCTGAGAAT and Tgfb2-GT-Re: TCCCTGGTACTGTTGTAGATGG. To identify the mutant allele, Tgfb2-mut-Fw: CGCTCAGTCTGTCTACCTCT and Tgfb2-GT-Re: TCCCTGGTACTGTTGTAGATGG primers were used. PCR conditions were: 94 °C for 2 min, 94 °C for 15 sec, 60 °C for 30 sec, 72 °C for 45 sec, steps 2–4 were repeated 34 times. Samples were stored at 4 °C. A typical gel used for genotyping is shown in Sup. Fig. 5.

Cell transfection

HEK293 cells (ATCC #CRL01573), expressing TGFβ2, TGFβ2^{C24S}, LTBP3, LTBP3 and TGFβ2 or LTBP3 and TGFβ2^{C24S} constructs, were generated by transiently transfection using Lipofectamine 2000. The following plasmids were used alone or in combination: LTBP3 – pEF6 hLTBP3myc2, containing a blasticidin resistance gene (gift of T. Nakamura); TGFβ2 – pEF6 hTGFβ2 (gift of R. Derynck); TGFβ2^{C24S}- pEF6 hTGFβ2^{C24S} generated using the Gibson assembly cloning kit (NEB#E5510S). Control cells were generated by transfection with empty vector – pEF6/myc2. After 16 h, the medium was changed to serum-free DMEM (GIBCO #11995-065). SF-CM was collected after 12 h incubation. SF-CM were either used directly for the measurement of TGFβ activity or concentrated 10-fold using centrifugal filter units (Amicon Ultra-4 #UFC800324) for analysis of protein levels.

Primary fibroblasts

Pregnant (E14.5) females were sacrificed, and the embryos removed from the uterine horns by dissection. Each embryo was separated from its placenta and embryonic sac in a tissue culture hood under aseptic conditions. Embryos were briefly rinsed in 70 % ethanol followed by PBS. A piece of tail/limb was saved for genotyping. Head and limbs were removed, and an incision was made at the midline of the abdomen from head to tail. All the internal organs were carefully removed. Tissues were finely minced using a sterile razor blade in a 100 mm dish in 1 ml 0.05 % trypsin, 0.053 mM EDTA (CORNING#25-052-CI) and transferred to a 1.5 ml tube for incubation for 15 m at 37 °C. Every 15 m, cells were pipetted up and down to dissociate the tissue. After one h, trypsin was inactivated by adding DMEM with 10 % FBS (GIBCO #16140-063). Cells were centrifuged at 400*g* for 5 m. The cell pellet was resuspended in 2 ml of DMEM with 10 % FBS. Cells were plated in two 10 cm plates per embryo and the following day, fresh DMEM with 10 % FBS (Day 0) was added. Cultures consisting primarily of fibroblasts were fully confluent by Day 3 [32]. Cells were immediately used for experiments or frozen for further use.

Measurement of total TGFβ

Measurement of total TGFβ was performed using a luciferase reporter cell assay as previously reported [33]. Luciferase activity is reported as relative light units (RLU). To detect TGFβ2 activity, SF-CM was activated by heat treatment. Recombinant TGFβ1 (cat#7754-BH/CF; lot# DCPU1223042), recombinant TGFβ2 (cat#302-B2; lot# KF 1918091), anti TGFβ1 (AF-101-SP) and anti TGFβ2 (AB-12-NA) were obtained from R&D. Antibody 1D11 was a generous gift from Genyzme Corp.

Western blot analysis for secreted TGFβ2 LAP/LLC/LTBP3

Confluent cultures of HEK293 cells overexpressing TGFβ2 or TGFβ2^{C24S} with or without LTBP3 were washed, cells were overlaid with serum free-DMEM, and the SF-CM collected after 24 h followed by clarification by centrifugation. Equal volumes of SF-CM from reduced or nonreduced samples were separated on 4–20 % mini-PROTAN TGX gels (BIO-RAD #4561094). After separation, proteins were transferred to methanol charged PVDF membranes. After transfer, membranes were blocked with 5 % Blotting-Grade blocker (BIO-RAD #1706404) in PBS/0.05 % Tween 20 and probed for 12–16 h at 4 °C with rabbit antibodies against LTBP3 or TGFβ2 LAP at a dilution of 1:1000 in blocking buffer (LI-COR #927-80001). Immunoreactive bands were visualized using ECL select western blotting detection chemiluminescent substrate (Amersham #RPN2235).

Immunohistochemistry and immunostaining

5 μm sections of fresh formalin-fixed tissues were used. All sections were stained with hematoxylin and eosin unless stated otherwise. For staining of TGFβ2 LAP, primary antibody (anti-LAP-TGFB2) was diluted 1:100 in 1XPBS and samples incubated in the diluted antibody for overnight at 4C. The next day, samples were washed 3 times in PBS at 5 m intervals and incubated with secondary antibody, goat anti-Rabbit Alexa 555 (Invitrogen #A-21428), at a dilution of 1:200 at room temperature. Immunofluorescence of pSmad2 (Invitrogen #44-244G) was performed as described by Sachan et al. [34]. For detection of TGFβ2 LAP immunofluorescence, antigen retrieval was performed using Dako target retrieval solution (Agilent Dako #S1700) for 3 m at 95 °C. Sections were washed twice with 1XPBS at 5 m intervals followed by 20 m incubation in Fc receptor blocker (Innovex biosciences #NB309-5S) and 20 m treatment in Background Buster (Innovex biosciences #NB306-7). All samples were washed 3 times at intervals of 5 mins with PBS and mounted with ProLong™ Gold Antifade Mountant with DAPI (Invitrogen #P36931). Images were acquired using Zeiss LSM760 confocal microscope.

Quantitation of Nuclear pSmad2: Image J (Fiji) software was used to perform the quantitation of nuclear pSmad3. Images were opened through the Bio-Formats Import selecting the 'hyperstack', 'colorized' and 'split channel' options. This allowed the independent analysis of the fluorescent channels for nuclear DAPI and nuclear pSmad2. Threshold of DAPI was adjusted and watershed was used if nuclei overlapped. All the nuclei were selected and saved with the.roi extension. The threshold of pSmad2 panel was then adjusted and all nuclei expressing pSmad3 were selected. The integrated density and standard deviation are shown in Sup. Fig. 5.

CRediT authorship contribution statement

Nalani Sachan: Writing – review & editing, Writing – original draft, Methodology, Investigation, Formal analysis, Conceptualization. **Colin K.L. Phoon:** Writing – review & editing, Methodology. **Lei Bu:** Writing –

review & editing, Methodology. **Lior Zilberberg:** Writing – review & editing, Methodology. **Jasimuddin Ahamed:** Writing – review & editing, Visualization, Funding acquisition. **Daniel B. Rifkin:** Writing – review & editing, Writing – original draft, Visualization, Supervision, Resources, Investigation, Funding acquisition, Formal analysis, Conceptualization.

Declaration of competing interest

The authors declare the following financial interests/personal relationships which may be considered as potential competing interests: Daniel B Rifkin reports financial support was provided by National Heart Lung and Blood Institute. Jasimuddin Ahamed reports financial support was provided by National Heart Lung and Blood Institute. If there are other authors, they declare that they have no known competing financial interests or personal relationships that could have appeared to influence the work reported in this paper.

Data availability

Data will be made available on request.

Acknowledgements

We acknowledge the use of the New York University Langone Medical Center (NYUMC) Histopathology and Transgenic Mouse Cores supported by NYUMC Cancer Center Grant P30CA016087, National Institutes of Health. This work was also supported, in part, by and was performed at the Preclinical Imaging laboratory supported by the Laura and Isaac Perlmutter Cancer Center Support Grant NCI SP30CA016087 and NIBIB Biomedical Technology Resource Center Grant NIH P41 E8017183. We thank Taylor Ene and Esme Zediker for assistance in genotyping of mice.

Author contributions

NS, LB CKLP, JA, and DBR collected and analyzed the data. NS, JA, and DBR wrote the manuscript. JA and DBR acquired funding. All authors read and revised the paper.

Funding

This work was supported by a grant P01 HL134605 from the National Heart, Lung, and Blood Institute to DBR and R01HL148123 and R01HL167656 to JA.

References

[1] M. Morikawa, R. Derynck, K. Miyazono, TGF-beta and the TGF-beta family: context-dependent roles in cell and tissue physiology, Cold Spring Harb. Perspect. Biol. 8 (2016).
[2] I.B. Robertson, D.B. Rifkin, Unchaining the beast; insights from structural and evolutionary studies on TGFbeta secretion, sequestration, and activation, Cytokine Growth Factor Rev. 24 (2013) 355–372.
[3] I.B. Robertson, D.B. Rifkin, Regulation of the bioavailability of TGF-beta and TGF-beta-related proteins, Cold Spring Harb. Perspect. Biol. 8 (2016).
[4] D.B. Constam, Regulation of TGFbeta and related signals by precursor processing, Semin. Cell Dev. Biol. 32 (2014) 85–97.
[5] S. Lienart, R. Merceron, C. Vanderaa, F. Lambert, D. Colau, J. Stockis, B. van der Woning, H. De Haard, M. Saunders, P.G. Coulie, S.N. Savvides, S. Lucas, Structural basis of latent TGF-beta1 presentation and activation by GARP on human regulatory T cells, Science 362 (2018) 952–956.
[6] Y. Qin, B.S. Garrison, W. Ma, R. Wang, A. Jiang, J. Li, M. Mistry, R.T. Bronson, D. Santoro, C. Franco, D.A. Robinton, B. Stevens, D.J. Rossi, C. Lu, T.A. Springer, A milieu molecule for TGF-beta required for microglia function in the nervous system, Cell 174 (2018) 156–171 e116.
[7] T. Harel, E. Levy-Lahad, M. Daana, H. Mechoulam, S. Horowitz-Cederboim, M. Gur, V. Meiner, O. Elpeleg, Homozygous stop-gain variant in LRRC32, encoding a TGFbeta receptor, associated with cleft palate, proliferative retinopathy, and developmental delay, Eur. J. Hum. Genet. 27 (2019) 1315–1319.
[8] D. Rifkin, N. Sachan, K. Singh, E. Sauber, G. Tellides, F. Ramirez, The role of LTBPs in TGF beta signaling, Dev. Dyn. 251 (2022) 95–104.
[9] M. Shi, J. Zhu, R. Wang, X. Chen, L. Mi, T. Walz, T.A. Springer, Latent TGF-beta structure and activation, Nature 474 (2011) 343–349.
[10] J. Ahamed, N. Burg, K. Yoshinaga, C.A. Janczak, D.B. Rifkin, B.S. Coller, In vitro and in vivo evidence for shear-induced activation of latent transforming growth factor-beta1, Blood 112 (2008) 3650–3660.
[11] J.S. Munger, D. Sheppard, Cross talk among TGF-beta signaling pathways, integrins, and the extracellular matrix, Cold Spring Harb. Perspect. Biol. 3 (2011) a005017.
[12] J. Saharinen, J. Keski-Oja, Specific sequence motif of 8-Cys repeats of TGF-beta binding proteins, LTBPs, creates a hydrophobic interaction surface for binding of small latent TGF-beta, Mol. Biol. Cell 11 (2000) 2691–2704.
[13] J.P. Annes, D.B. Rifkin, J.S. Munger, The integrin alphaVbeta6 binds and activates latent TGFbeta3, FEBS Lett. 511 (2002) 65–68.
[14] J.S. Munger, X. Huang, H. Kawakatsu, M.J. Griffiths, S.L. Dalton, J. Wu, J.F. Pittet, N. Kaminski, C. Garat, M.A. Matthay, D.B. Rifkin, D. Sheppard, The integrin alpha v beta 6 binds and activates latent TGF beta 1: a mechanism for regulating pulmonary inflammation and fibrosis, Cell 96 (1999) 319–328.
[15] B. Hinz, The extracellular matrix and transforming growth factor-beta1: Tale of a strained relationship, Matrix Biol. 47 (2015) 54–65.
[16] X. Dong, B. Zhao, R.E. Iacob, J. Zhu, A.C. Koksal, C. Lu, J.R. Engen, T.A. Springer, Force interacts with macromolecular structure in activation of TGF-beta, Nature 542 (2017) 55–59.
[17] D. Mu, S. Cambier, L. Fjellbirkeland, J.L. Baron, J.S. Munger, H. Kawakatsu, D. Sheppard, V.C. Broaddus, S.L. Nishimura, The integrin alpha(v)beta8 mediates epithelial homeostasis through MT1-MMP-dependent activation of TGF-beta1, J. Cell Biol. 157 (2002) 493–507.
[18] M.G. Campbell, A. Cormier, S. Ito, R.I. Seed, A.J. Bondesson, J. Lou, J.D. Marks, J. L. Baron, Y. Cheng, S.L. Nishimura, Cryo-EM reveals integrin-mediated TGF-beta activation without release from latent TGF-beta, Cell 180 (2020) 490–501 e416.
[19] Z. Yang, Z. Mu, B. Dabovic, V. Jurukovski, D. Yu, J. Sung, X. Xiong, J.S. Munger, Absence of integrin-mediated TGFbeta1 activation in vivo recapitulates the phenotype of TGFbeta1-null mice, J. Cell Biol. 176 (2007) 787–793.
[20] K. Yoshinaga, H. Obata, V. Jurukovski, R. Mazzieri, Y. Chen, L. Zilberberg, D. Huso, J. Melamed, P. Prijatelj, V. Todorovic, B. Dabovic, D.B. Rifkin, Perturbation of transforming growth factor (TGF)-beta1 association with latent TGF-beta binding protein yields inflammation and tumors, PNAS 105 (2008) 18758–18763.
[21] R. Wang, J. Zhu, X. Dong, M. Shi, C. Lu, T.A. Springer, GARP regulates the bioavailability and activation of TGFbeta, Mol. Biol. Cell 23 (2012) 1129–1139.
[22] V.Q. Le, B. Zhao, S. Ramesh, C. Toohey, A. DeCosta, J. Mintseris, X. Liu, S. Gygi, T. A. Springer, A specialized integrin-binding motif enables proTGF-beta2 activation by integrin alphaVbeta6 but not alphaVbeta8, PNAS 120 (2023) e2304874120.
[23] M. Azhar, J. Schultz Jel, I. Grupp, G.W. Dorn 2nd, P. Meneton, D.G. Molin, A. C. Gittenberger-de Groot, T. Doetschman, Transforming growth factor beta in cardiovascular development and function, Cytokine Growth Factor Rev. 14 (2003) 391–407.
[24] L.P. Sanford, S. Kallapur, I. Ormsby, T. Doetschman, Influence of genetic background on knockout mouse phenotypes, Methods Mol. Biol. 158 (2001) 217–225.
[25] L.P. Sanford, I. Ormsby, A.C. Gittenberger-de Groot, H. Sariola, R. Friedman, G. P. Boivin, E.L. Cardell, T. Doetschman, TGFbeta2 knockout mice have multiple developmental defects that are non-overlapping with other TGFbeta knockout phenotypes, Development 124 (1997) 2659–2670.
[26] N.F. Brown, J.F. Marshall, Integrin-mediated TGFbeta activation modulates the tumour microenvironment, Cancers (Basel) 11 (2019).
[27] L. Ivanov II, N. Frutos Rde, K. Manel, D.B. Yoshinaga, R.B. Rifkin, B.B. Sartor, D.R. L. Finlay, Specific microbiota direct the differentiation of IL-17-producing T-helper cells in the mucosa of the small intestine, Cell Host Microbe 4 (2008) 337–349.
[28] Y. Yokosaki, N. Matsuura, S. Higashiyama, I. Murakami, M. Obara, M. Yamakido, N. Shigeto, J. Chen, D. Sheppard, Identification of the ligand binding site for the integrin alpha9 beta1 in the third fibronectin type III repeat of tenascin-C, J. Biol. Chem. 273 (1998) 11423–11428.
[29] X.Z. Huang, J.F. Wu, R. Ferrando, J.H. Lee, Y.L. Wang, R.V. Farese Jr., D. Sheppard, Fatal bilateral chylothorax in mice lacking the integrin alpha9beta1, Mol. Cell Biol. 20 (2000) 5208–5215.
[30] J.P. Annes, Mechanism of Latent TGF-beta Activation, Ph.D. thesis, (2003).
[31] M. Azhar, K. Brown, C. Gard, H. Chen, S. Rajan, D.A. Elliott, M.V. Stevens, T. D. Camenisch, S.J. Conway, T. Doetschman, Transforming growth factor Beta2 is required for valve remodeling during heart development, Dev. Dyn. 240 (2011) 2127–2141.
[32] A. Nagy, M. Gertsenstein, K. Vintersten, R. Behringer, Preparing mouse embryo fibroblasts, CSH Protoc 2006 (2006).
[33] M. Abe, J.G. Harpel, C.N. Metz, I. Nunes, D.J. Loskutoff, D.B. Rifkin, An assay for transforming growth factor-beta using cells transfected with a plasminogen activator inhibitor-1 promoter-luciferase construct, Anal. Biochem. 216 (1994) 276–284.
[34] N. Sachan, C.K.L. Phoon, L. Zilberberg, M.C. Kugler, T. Ene, S.B. Mintz, S. I. Murtada, D. Weiss, G.I. Fishman, J.D. Humphrey, D.B. Rifkin, TGFbeta-2 haploinsufficiency causes early death in mice with Marfan syndrome, Matrix Biol. (2023).